RADIATIVE CORRECTIONS TO $e^+e^- \to$ HADRONS $+ \gamma$ AND $e^+e^- \to \mu^+\mu^- + \gamma^*$

Szymon Tracz

Instituto de Física Corpuscular
Universitat de Valencia — Consejo Superior de Investigaciones Científicas
Parc Científic, 46980 Paterna, Valencia, Spain

The review of the recent developments in the field of radiative corrections and their implementation in the Monte Carlo event generator Phokhara is presented. Furthermore, discussion of the importance of obtained results for future measurements of the hadronic cross section is performed.

1. Introduction

One of the most important observables in particle physics is the hadronic cross section. It constitutes important input for the parameters used in tests of the Standard Model and its extensions. Its value governs the running of the electromagnetic coupling constant at low energy up to the mass of Z^0 boson and is, therefore, very important for the precision of analysis of the electroweak interaction. It constitutes the crucial input for determination of strong coupling constant, quark masses, Z^0 mass, and its width and low-energy quantities such as pion or nucleon form factors. Furthermore, the hadronic cross section is very important for a precise determination of the muon anomalous magnetic moment $(g-2)_\mu$. The physical quantity, which experimental value deviates from the Standard Model predictions more than 3σ [1, 2]. The error of this discrepancy is dominated by the hadronic contributions [1, 2], which cannot be calculated perturbatively with desired precision. One of the crucial contributions to the hadronic part comes from the hadronic vacuum polarization (HVP) diagrams. This contribution can be calculated using dispersive integral approach, which relates the HVP to

---

the measured value of the $e^+e^- \to$ hadrons cross section. As the error of the Monte Carlo event generators used for data analysis constitutes part of the systematic uncertainty of the measurement, including higher order radiative corrections is necessary to ensure the appropriate precision of the simulations. The dominant contribution to the HVP part and its uncertainty come from the pion-pair production. Its precise determination is limited by the observed discrepancy between BaBar and KLOE measurements [3]. As this discrepancy might have originated partly from the missing radiative corrections, including the higher order effects in the data analysis may help to resolve this issue. On the other hand, the $e^+e^- \to \mu^+\mu^-\gamma$ reaction can also influence the precise determination of the hadronic cross section. This reaction is often used for monitoring the luminosity and, therefore, introduces an additional contribution to the systematic error of the experiment.

In these proceedings, we report on the latest upgrade of the Monte Carlo event generator Phokhara [4, 5]. In Section 2, we review the information about the radiative return method. In Section 3, we describe the contributions to the reactions $e^+e^- \to$ hadrons $+ \gamma$ and $e^+e^- \to \mu^+\mu^- + \gamma$ at the next-to-leading order (NLO) and beyond. Then, in Sections 4 and 5, the most important developments are discussed, the complete NLO radiative corrections for $\pi^+\pi^-\gamma$ channel and NNLO initial-state corrections to the radiative return cross section.

2. Radiative return method

One of the possibilities to measure the hadronic cross section is based on the radiative return method [6, 7]. In this approach, the cross section with the emission of a photon(s) from an initial state can be cast into the following form:

$$\mathrm{d}\sigma(e^+e^- \to \text{hadrons} + \gamma_{\mathrm{ISR}})\left(Q^2\right) = H\left(Q^2, \theta_\gamma\right) \mathrm{d}\sigma(e^+e^- \to \text{hadrons})\left(Q^2\right),$$
(1)

where $H(Q^2, \theta_\gamma)$ is a radiator function, which depends on the invariant mass of the final state — Q^2, and polar angles of emitted photon(s) θ_γ.

This method allows measuring hadronic cross section over the wide range of energies, from the threshold for production of a given final state up to the nominal energy of the experiment. The radiator function is fully calculable within QED but its precise knowledge involves the calculation of radiative corrections. Moreover, relation (1) holds only for the photons emitted from the initial state (ISR), so the contributions from the diagrams, where photons are emitted from the final state (FSR) have to be subtracted. The size of the FSR can be suppressed by suitable experimental cuts. In general, ISR is enhanced for the events, where photons are emitted at small angles and FSR is suppressed for events, where photons are geometrically well-separated

from the final-state particles. The more extensive discussions of the impact of the FSR for the radiative return and method for testing its models can be found in [7, 8]. The FSR contributions have to be well-controlled in experiments. In practice, due to the complicated experimental setup, the size of the FSR corrections is taken from the Monte Carlo event generators. For the purpose of measurement of the hadronic cross section, the Phokhara Monte Carlo event generator has been constructed [4, 5]. This generator is based on reliable models of the FSR corrections for multihadronic final states, which have been well-tested experimentally.

3. Radiative return at the the next-to-leading order and beyond

Assuming that the final state consists of a particle–antiparticle pair, in fact, the production of $\mu^+ \mu^-$ or $\pi^+ \pi^-$ will be considered, the leading order (LO) amplitude for the reaction $e^+(p_1)e^-(p_2) \to f(Q^2) + \gamma(k_1)$ is given by the coherent sum of ISR and FSR amplitudes

$$\mathcal{M}_{\mathrm{LO}} = \mathcal{M}_{\mathrm{ISR}} + \mathcal{M}_{\mathrm{FSR}}, \qquad (2)$$

where $f(Q^2)$ represents the hadronic or leptonic final state with invariant mass Q^2 and $(p_1 + p_2)^2 = \sqrt{s}$. The classes of diagrams, which contribute to the leading order cross section are presented in Fig. 1. Complete result for the LO cross section, which takes into account the FSR and its interference with the ISR can be found in [7, 9]. The finiteness of the leading order cross section is ensured by requiring minimal energy of the emitted photon, defined by the parameter g_{min}.

a)   b)
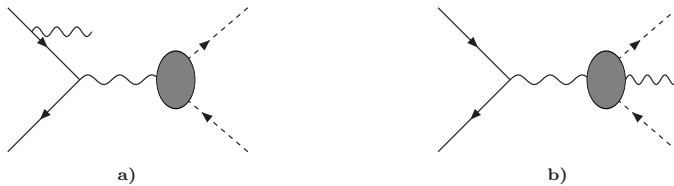
Fig. 1. The classes of diagrams with the emission of one photon, which contribute to the reaction $e^+e^- \to f(Q^2) + \gamma$ at the LO. The $\pi^+\pi^-$ final state is assumed and blob represents modeling of the pion–antipion–photon interaction.

At the next-to-leading order (NLO), one has to include one-loop corrections from Fig. 2 and diagrams with the emission of one additional hard photon presented in Fig. 3. The complete set of one-loop corrections includes diagrams with vertex, self-energy corrections, and corrections, which include the exchange of two virtual photons between initial and final states. Additionally, one has also to take into account the contributions from diagrams with one soft ($E_\gamma < E_{\mathrm{min}}$) and one hard photon ($E_\gamma > E_{\mathrm{min}}$). Only

the sum of virtual and soft corrections makes the total cross section infrared finite. The independence of the total cross section on the separation parameter ($w = E_{\min}/\sqrt{s}$), between soft and hard photon's phase-space regions, is obtained by including additional contributions from diagrams with two hard photons, where energies of both photons fulfill the condition of $E_\gamma > E_{\min}$. The classes of diagrams for pions and muons are the same, the only difference is that within a given class, additional topology, where two photons couple to the final particle–antiparticle pair have to be taken into account, in the pion case. A more detailed discussion of specific contributions is presented in [10] for muons and in [11] for pions.
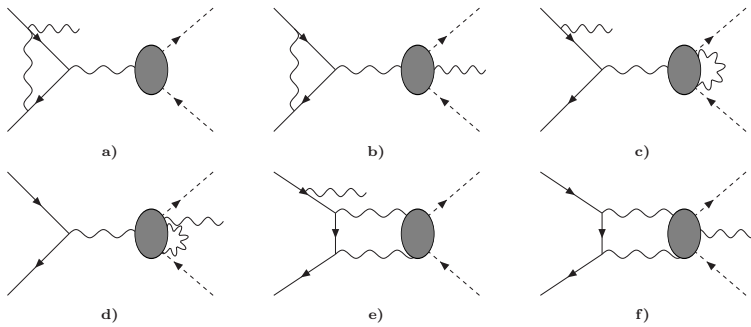
Fig. 2. The classes of virtual corrections, which contribute to the reaction $e^+e^- \to f(Q^2) + \gamma$ at the NLO. The $\pi^+\pi^-$ final state is assumed and blob represents modeling of the pion–antipion–photon interaction.
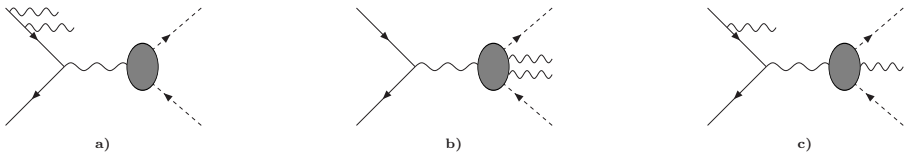
Fig. 3. The classes of diagrams with the emission of two photons, which contribute to the radiative return cross section at the NLO. The $\pi^+\pi^-$ final state is assumed and blob represents modeling of the pion–antipion–photon interaction.

The complete differential cross section at the NLO can be written in the following form:

$$\mathrm{d}\sigma_{\mathrm{NLO}} = \mathrm{d}\sigma_{1\gamma,\mathrm{LO}} + \mathrm{d}\sigma_{1\gamma,\mathrm{NLO}} + \mathrm{d}\sigma_{2\gamma}, \tag{3}$$

where the LO cross section is given by the following formula:

$$\mathrm{d}\sigma_{1\gamma,\mathrm{LO}} = \frac{1}{2s}|\mathcal{M}_{\mathrm{LO}}|^2 \mathrm{d}\phi_2\left(Q, q_1, q_2\right) \mathrm{d}\phi_2\left(p_1, p_2; Q, k_1\right) \frac{\mathrm{d}Q^2}{2\pi}, \tag{4}$$

where $\mathrm{d}\phi_2(Q; q_1, q_2)$ denotes 2-body hadronic (muonic) phase-space element, which has the following form:

$$\mathrm{d}\phi_2 \left(Q; q_1, q_2\right) = \frac{1}{32\pi^2}\sqrt{1 - \frac{4m_{\mathrm{f}}^2}{Q^2}}\,\mathrm{d}\Omega\,, \tag{5}$$

where $\mathrm{d}\Omega$ is the solid angle of one of the final-state particles and m_{f} is its mass. The 2-body phase-space element $\mathrm{d}\phi_2(p_1, p_2; Q, k_1)$, which depends on photon momenta k_1 has the following form:

$$\mathrm{d}\phi_2 \left(p_1, p_2; Q, k_1\right) = \frac{1}{32\pi^2}\left(1 - \frac{Q^2}{s}\right)\mathrm{d}\Omega_1\,, \tag{6}$$

where $\mathrm{d}\Omega_1$ is the solid angle of the photon. The one-photon cross section at the NLO is given by the following formula:

$$\begin{aligned}
\mathrm{d}\sigma_{1\gamma,\mathrm{NLO}} &= \frac{1}{2s}\left(2\mathcal{R}e\left(\mathcal{M}_{\mathrm{LO}}\mathcal{M}_{\mathrm{NLO}}^\dagger\right) + |\mathcal{M}_{\mathrm{1s,1h}}|^2\right) \\
&\quad \times \mathrm{d}\phi_2\left(Q, q_1, q_2\right)\mathrm{d}\phi_2\left(p_1, p_2; Q, k_1\right)\frac{\mathrm{d}Q^2}{2\pi}\,.
\end{aligned} \tag{7}$$

The matrix element $\mathcal{M}_{\mathrm{NLO}}$ includes virtual corrections presented in Fig. 2 and $\mathcal{M}_{\mathrm{1s,1h}}$ represents contributions from the diagrams presented in Fig. 3, where one photon is soft and one hard. The complete NLO corrections for the muon case were calculated in [10], while dominant contributions have been already presented in [4, 9, 12]. In the case of pions, the result of complete NLO corrections can be found in [11], while the partial results have been published in [4, 9, 13].

The two-photon cross section is given by the following formula:

$$\mathrm{d}\sigma_{2\gamma} = \frac{1}{2s}|\mathcal{M}_{2\gamma}|^2\mathrm{d}\phi_2\left(Q, q_1, q_2\right)\mathrm{d}\phi_3\left(p_1, p_2; Q, k_1, k_2\right)\frac{\mathrm{d}Q^2}{2\pi}\,. \tag{8}$$

The matrix element $\mathcal{M}_{2\gamma}$ includes all possible contributions with the emission of two photons, where photons can be emitted either from the initial or final state. The calculation of the matrix element with the emission of two hard photons from the initial state has been already presented in [9]. The dominant FSR contributions, where one of the photons is emitted from the

initial and one from the final state is presented in [12]. The result of the calculation of the double real emission from the final state can be found in [10] for muons and in [11] for pions.

The element of the phase space, which depends on photons momenta k_1 and k_2, written in the center-of-mass system (CMS) of electron–positron is given by the following formula [9]:

$$\mathrm{d}\phi_3\left(p_1, p_2; Q, k_1, k_2\right) = \frac{1}{2!}\frac{s}{4(2\pi)^5}\frac{w_1 w_2^2}{1 - q^2 - 2w_1}\mathrm{d}w_1\,\mathrm{d}\Omega_1\,\mathrm{d}\Omega_2\,, \qquad (9)$$

with $q^2 = Q^2/s$, $w_i = E_i/\sqrt{s}$, where E_i and $\mathrm{d}\Omega_i$ are photons energies and solid angles.

The squares of the matrix elements $\mathcal{M}_{i\gamma}$ contain several peaks, which could lead to inefficient Monte Carlo generation. These peaks are softened by a suitable change of integration variables. The change of variables for one and two photons has been described in [9].

The energies of all photons have to be bigger than minimal photon energy defined by the soft-photon cutoff $w = E_{\min}/\sqrt{s}$. The total cross section should be independent of this parameter, yet this parameter is indispensable for the Monte Carlo generation. The soft-photon approximation requires w value to be small but too small value could lead to the negative weights. In the numerical simulation the usual value of w is 10^{-4}–10^{-5}. Additionally, experimental conditions for radiative return require that at least one emitted photon need to have energy $E_i > g_{\min}$, where $g_{\min}$ is determined by the experiment event selections.

The first step to include radiative corrections to the reaction $e^+e^- \to \gamma^*(Q^2) + \gamma$ beyond the NLO is to include dominant contributions in the framework of leading logarithmic approximation [14]. Considered corrections affect only the initial state, so the virtual photon $\gamma^*(Q^2)$ can decay to an arbitrary final state. The NNLO cross section of the reaction can be written in the following form:

$$\begin{aligned}\sigma_{\mathrm{NNLO}} = {} & \left(\Delta_{\mathrm{soft,1ph}} + \Delta_{\mathrm{virt,1ph}}\right)\sigma_{1\gamma_{\mathrm{ISR}}} \\ & + \left(\Delta_{\mathrm{soft,2ph}} + \Delta_{\mathrm{virt,soft,1ph}} + \Delta_{\mathrm{virt,2ph}}\right)\sigma_{2\gamma_{\mathrm{ISR}}} + \sigma_{3\gamma_{\mathrm{ISR}}}\,, \quad (10)\end{aligned}$$

where $\sigma_{i\gamma_{\mathrm{ISR}}}$ represents cross section with emission of i hard photons. For $\sigma_{1\gamma_{\mathrm{ISR}}}$ and $\sigma_{2\gamma_{\mathrm{ISR}}}$ the appropriate contributions can be extracted from Eqs. (4) and (8). The classes of the diagrams, which represent possible contributions to the radiative return cross section at the NNLO are presented in Fig. 4. The leading logarithmic terms of virtual and soft corrections according to [15] are given by the following formulae:

$$\Delta_{\mathrm{soft,1ph}} = \frac{\alpha}{\pi}\left(\log\left(s/m_e^2\right) - 1\right)\log(2w)\,, \qquad (11)$$
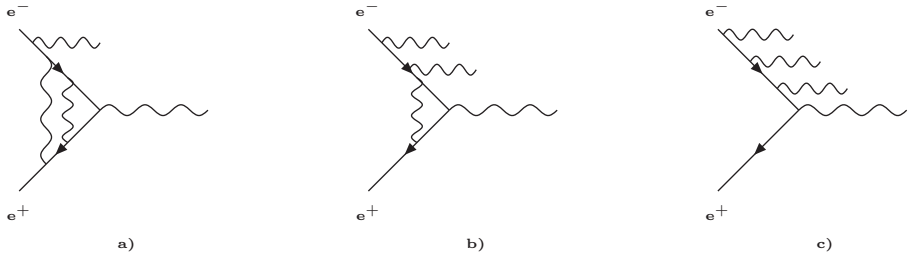
Fig. 4. Possible contributions to the cross section for the reaction $e^+e^- \to \gamma^*(Q^2) + \gamma$ at the NNLO.

$$\Delta_{\text{virt,1ph}} = \frac{3\alpha}{2\pi} \log\left(Q^2/m_e^2\right) , \tag{12}$$

$$\Delta_{\text{soft,2ph}} = \frac{\Delta_{\text{soft,1ph}}^2}{2} , \tag{13}$$

$$\Delta_{\text{virt,soft,1ph}} = \Delta_{\text{soft,1ph}}\Delta_{\text{virt,1ph}} , \tag{14}$$

$$\Delta_{\text{virt,2ph}} = \frac{9\alpha}{8\pi} \log^2\left(Q^2/m_e^2\right) . \tag{15}$$

The cross section for the emission of three hard photons ($\sigma_{3\gamma\text{ISR}}$), where $\gamma^*(Q^2)$ decays into j particles can be written in the following form:

$$\sigma_{3\gamma\text{ISR}} = \frac{1}{2s}|M_{3\gamma\text{ISR}}|^2 \frac{1}{2\pi^2} \mathrm{d}Q^2 \, \mathrm{d}\phi_4\left(p_1, p_2; Q, k_1, k_2, k_3\right) \mathrm{d}\phi_j\left(Q; q_1, \ldots q_j\right) , \tag{16}$$

where $\mathrm{d}\phi_j(Q; q_1, \ldots q_j)$ depends on the number of final-state particles and reduces to Eq. (5) in the case of $j = 2$. The matrix element $M_{3\gamma\text{ISR}}$ has been calculated using helicity amplitude method [16, 17]. It includes the set of 24 diagrams of the class presented in Fig. 4 (c). The element of the phase space, which depends on the momenta of three photons, in the CMS of electron–positron can be written in the following form:

$$\mathrm{d}\phi_4\left(p_1, p_2; Q, k_1, k_2, k_3\right) = \frac{s^2}{16(2\pi)^8}$$
$$\times \frac{2w_1 w_2 w_3^2 \, \mathrm{d}w_1 \, \mathrm{d}w_2 \, \mathrm{d}\Omega_1 \, \mathrm{d}\Omega_2 \, \mathrm{d}\Omega_3}{1 - q^2 - 2w_1 - 2w_2 + 2w_1 w_2(1 - \cos\theta_{12})} , \tag{17}$$

where E_i and $\mathrm{d}\Omega_i$ are photons energies and solid angles, and as in the case of two photons, we use scaled variables q^2 and w_i. The soft and collinear peaks, which appear in the square of the matrix element $M_{3\gamma\text{ISR}}$ were absorbed into the change of variables similarly as it was done in the case of two photons [9].

4. Complete NLO radiative corrections
to the reaction $e^+e^- \to \pi^+\pi^-\gamma$

The current knowledge of the pionic contribution to the $(g-2)_\mu$ is limited by the discrepancy observed between KLOE and BaBar data for extraction of the pion form factor [3]. Both of these experiments used Phokhara Monte Carlo event generator for data analysis. This generator was based on approximate NLO radiative corrections. Given this, the possible impact of missing complete NLO radiative corrections for the reaction $e^+e^- \to \pi^+\pi^-\gamma$ has to be investigated. The missing contributions include diagrams from Fig. 2 (d)–(f) with appropriate soft-photon emissions and double real emission from the final state presented in Fig. 3 (b). Since KLOE [3, 18–20] and BaBar [21, 22] used different event selections, the different impact of the radiative corrections can be expected. The possible reason for this discrepancy caused by the missing radiative corrections in the case of $\mu^+\mu^-\gamma$ channel has been discussed in [10]. It has been shown that corrections, which were not previously included are not the origin of the observed experimental discrepancy.

The complete NLO radiative corrections to the $e^+e^- \to \pi^+\pi^-\gamma$ reaction have been calculated [5, 11], where for virtual corrections, the method described in [23–25] has been used. The soft-photon contributions have been calculated according to [26] and two hard-photon amplitudes using helicity amplitude method. More details about these calculations will be presented in [11]. Obtained results for experimental event selections show that the size of the corrections, which were not present in the previous version of the Phokhara code [10] are below 0.5% in the relevant region for the experimental analysis [5]. As a consequence, the discrepancy between KLOE and BaBar measurements cannot be explained by the lack of complete NLO radiative corrections in the event generator Phokhara, and thus this discrepancy can be only of experimental origin.

5. ISR NNLO radiative corrections

The comparison between Phokhara and KKMC [27] Monte Carlo event generators, which was presented in [28], allowed to establish declared precision of Phokhara for the ISR corrections at the level of 0.5%. The difference between these generators is that KKMC uses exponentiation formula to sum leading higher order effects, while Phokhara is based on fixed order calculations. The KKMC generator cannot be used in the experimental analysis for radiative return, as the full information about the kinematics of emitted photon(s) is required and it does not include hadronic channels. The missing third order leading logarithmic corrections in Phokhara are mostly responsible for the observed deviation. One could expect that including ISR NNLO

corrections will lead to improving the precision of Phokhara up to the level of 0.1%–0.2%. This improvement is necessary as future experimental measurements of the $(g-2)_\mu$ will be performed by the FERMILAB and JPARC with the uncertainty about 4 times smaller. Given this, the improvement of the precision for theoretical calculations of the $(g-2)_\mu$ has to be done. This can be achieved by a more precise measurement of the hadronic cross section, especially the pionic one. One of the ways to improve the precision of this measurement is to reduce the systematic error, which comes from the Monte Carlo generators.

The third order leading logarithmic corrections have been implemented in Phokhara Monte Carlo event generator in the form presented in Eqs. (11)–(15). The contributions with the emission of three hard photons have been calculated with full kinematic dependencies using the helicity amplitude method. Obtained results confirmed predictions presented in [28]. The further analysis of the size of these corrections for realistic experimental event selections has to be done to investigate how experimental observables could be affected by considered additional contributions.

6. Conclusions

The current status of the calculations of the radiative corrections to the reactions $e^+e^- \to$ hadrons $+ \gamma$ and $e^+e^- \to \mu^+\mu^- + \gamma$, with emphasis on the most important pionic channel has been reviewed. The overview of the current level of precision and the status of the implementation of the radiative corrections into Phokhara Monte Carlo event generator has been given. The most important results and their impact on the hadronic cross section, especially the pionic one were summarized. Discussion of the recent results and future developments in the context of the observed discrepancy between Standard Model and experimental value of the $(g-2)_\mu$ was discussed.

REFERENCES

[1] A. Keshavarzi, D. Nomura, T. Teubner, *Phys. Rev. D* **97**, 114025 (2018).

[2] M. Davier, A. Hoecker, B. Malaescu, Z. Zhang, *Eur. Phys. J. C* **77**, 827 (2017).

[3] A. Anastasi *et al.*, *J. High Energy Phys.* **1803**, 173 (2018).

[4] H. Czyz, A. Grzelinska, J.H. Kühn, G. Rodrigo, *Eur. Phys. J. C* **27**, 563 (2003) .

[5] F. Campanario *et al.*, *Phys. Rev. D* **100**, 076004 (2019).

[6] M.-S. Chen, P.M. Zerwas, *Phys. Rev. D* **11**, 58 (1975).

[7] S. Binner, J.H. Kühn, K. Melnikov, *Phys. Lett. B* **459**, 279 (1999).

[8] A. Hoefer, J. Gluza, F. Jegerlehner, *Eur. Phys. J. C* **24**, 51 (2002).

[9] G. Rodrigo, H. Czyż, J.H. Kühn, M. Szopa, *Eur. Phys. J. C* **24**, 71 (2002).

[10] F. Campanario *et al.*, *J. High Energy Phys.* **1402**, 114 (2014).

[11] F. Campanario *et al.*, in preparation.

[12] H. Czyż, A. Grzelińska, J.H. Kühn, G. Rodrigo, *Eur. Phys. J. C* **39**, 411 (2005).

[13] H. Czyż, A. Grzelińska, J.H. Kühn, G. Rodrigo, *Eur. Phys. J. C* **33**, 333 (2004).

[14] M. Skrzypek, S. Jadach, *Z. Phys. C* **49**, 577 (1991).

[15] F.A. Berends, W.L. van Neerven, G.J.H. Burgers, *Nucl. Phys. B* **297**, 429 (1988) [*Erratum ibid.* **304**, 921 (1988)].

[16] F. Jegerlehner, K. Kołodziej, *Eur. Phys. J. C* **12**, 77 (2000).

[17] K. Kolodziej, M. Zralek, *Phys. Rev. D* **43**, 3619 (1991).

[18] D. Babusci *et al.*, *Phys. Lett. B* **720**, 336 (2013).

[19] F. Ambrosino *et al.*, *Phys. Lett. B* **700**, 102 (2011).

[20] F. Ambrosino *et al.*, *Phys. Lett. B* **670**, 285 (2009).

[21] B. Aubert *et al.*, *Phys. Rev. Lett.* **103**, 231801 (2009).

[22] J.P. Lees *et al.*, *Phys. Rev. D* **86**, 032013 (2012).

[23] A. Denner, S. Dittmaier, *Nucl. Phys. B* **734**, 62 (2006).

[24] T. Binoth *et al.*, *J. High Energy Phys.* **0510**, 015 (2005).

[25] F. Campanario, *J. High Energy Phys.* **1110**, 070 (2011).

[26] G. 't Hooft, M.J.G. Veltman, *Nucl. Phys. B* **153**, 365 (1979).

[27] S. Jadach, B.F.L. Ward, Z. Wąs, *Comput. Phys. Commun.* **130**, 260 (2000).

[28] S. Jadach, *Acta Phys. Pol. B* **36**, 2387 (2005).